SUPPORTING INFORMATION

A Photoactivatable Push-Pull Fluorophore for Single-Molecule Imaging in Live Cells

Samuel J. Lord, Nicholas R. Conley, Hsiao-lu D. Lee,
Reichel Samuel, Na Liu, Robert J. Twieg, W. E. Moerner
Department of Chemistry, Stanford University, Stanford, California 94305-5080
Department of Chemistry, Kent State University, Kent, Ohio 44240

Index

Table S1. Hammett substituent constants[a] for relevant groups at *para* position

	σ_p
–N_3	0.08
–NH_2	–0.66
–NO_2	0.78
–CN	0.66
–CH=C$(CN)_2$	0.84
–CH(CN)=C$(CN)_2$	0.98
–DCDHF[b]	+

[a] Positive values are electron-withdrawing substituents; negative are electron-donating. For more information, see section 8.3 of reference 1. Values are from reference 2.

[b] The Hammett values for the DCDHF acceptor moiety is unknown, but it is a known strong electron-accepting group; cyano, dicyanovinyl, and tricyanovinyl values are included for rough extrapolation.

Table S2. Photophysical properties[a]

	λ_{abs} (nm)	λ_{fl} (nm)	ε_{max} ($M^{-1}cm^{-1}$)	Φ_F	Φ_P[b]	Φ_B[c]	SM $N_{tot,e}$[d]
1	424	552	29,100	n/a	0.0059	n/a	n/a
2	570	613	54,100	0.025–0.39[e]	n/a	4.1×10^{-6}	7.2×10^{6} [2.3×10^{6}]
Dronpa[f]	503	518	95,000	0.85	~0.013	$\sim3.2\times10^{-5}$	
PA-GFP[g]	504	517	17,400	0.79	10^{-8}–10^{-6}	$\sim6.9\times10^{-5}$	~140,000
EYFP[h]	514	527	84,000	0.61	$\sim2\times10^{-5}$	5.5×10^{-5}	~140,000
Cy3/Cy5[i]	647	662	200,000	0.18	~0.04		~670,000
PC-RhB[j]	552	580	110,000	0.65	"low"		24,000–600,000

[a] see below for details on measurements and calculations; values for **1** and **2** reported in ethanol unless otherwise stated

[b] quantum yield of photoconversion from azide with 407-nm illumination using measured $\bar{\tau}_{PA}$; in the other systems, we calculated rough estimations from available information, such as irradiation time and intensity (see discussion below)

[c] bulk quantum yield of permanent photobleaching, measured in aqueous gelatin for **2** and as reported in references below for other systems

[d] average number of photons emitted per molecule in PMMA [gelatin] for **2**; estimated from references below for other systems

[e] fluorescence quantum yield in ethanol and PMMA; rigidification of host media increases the brightness[3]

[f] aqueous photophysical values for the reversibly photoswitchable GFP called Dronpa from references 4, 5

[g] aqueous and in-cell photophysical values for the irreversibly photoswitchable GFP called PA-GFP as reported in references 6–8

[h] photophysical values, as reported in references 7–10

[i] aqueous photophysical values of a Cy3/Cy5 dimer on hybridized DNA, as reported in references 7, 11

[j] photophysical values of a photoswitchable Rhodamine B embedded in a poly(vinyl alcohol) film, as reported in reference 12; the range of $N_{tot,e}$ values is for rhodamine 6G in water from reference 13 and tetramethyl rhodamine in lipid membranes from reference 7, respectively

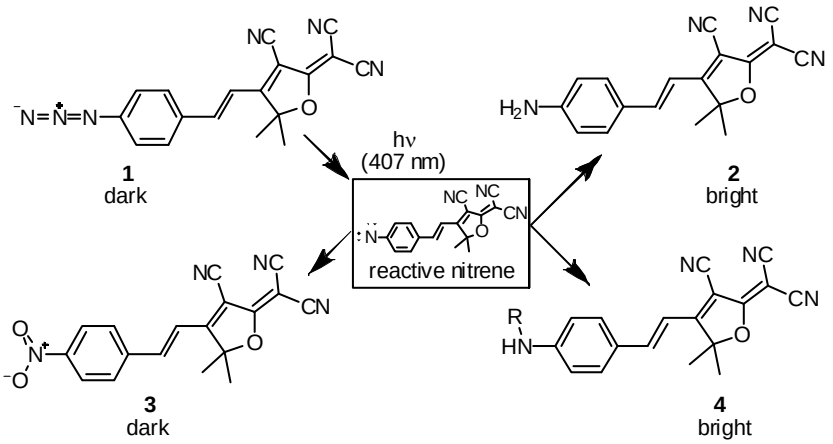

Scheme S1. Various products resulting from photochemical conversion of the azido-DCDHF fluorogen (**1**). Compounds **1**–**3** have been identified; **4** is hypothetical.

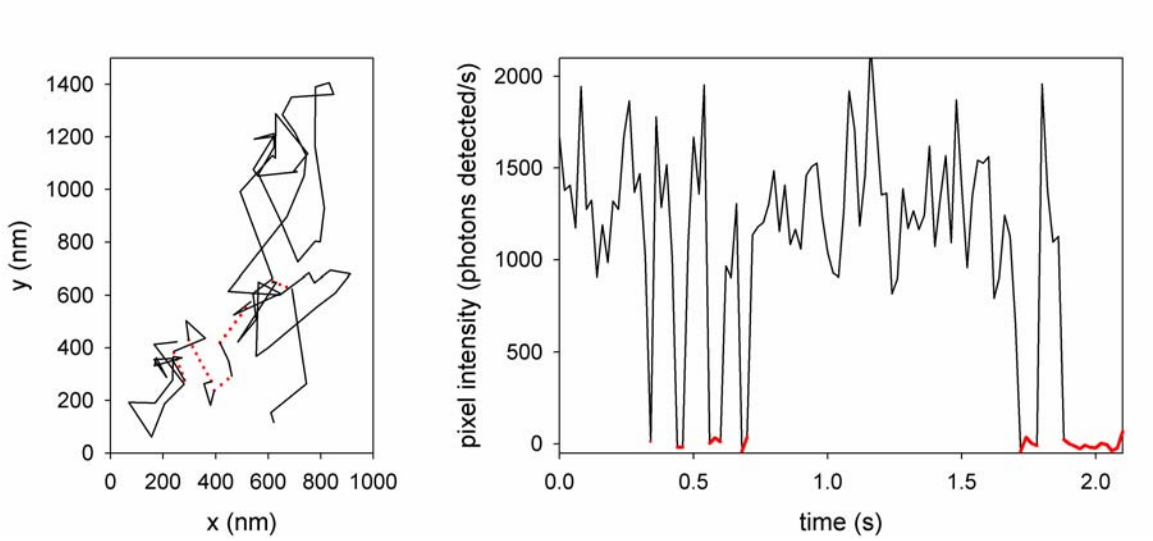

Figure S1. (*left*) The trajectory of a single copy of the DCDHF fluorophore diffusing in the membrane of a CHO cell after photoactivation. Dotted red lines indicate when the fluorophore was dark (i.e. blinking). (*right*) A background-subtracted intensity time-trace of the molecule in the trajectory on the left. Red lines indicate when the fluorophore was dark (i.e., initially blinking events, then finally bleaching). (See Movie S2.)

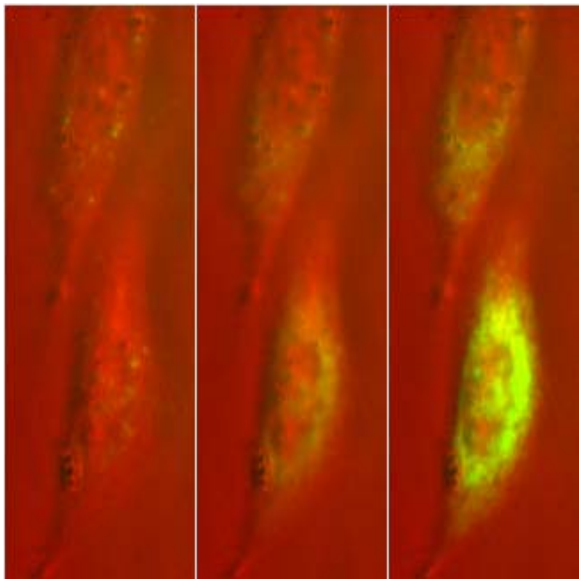

Figure S2. Two CHO cells (100×) incubated with fluorogen **1** before (*left*) activation and after one-second (*middle*) and five-second (*right*) flashes of diffuse, moderate-irradiance (13 W/cm^2) 407-nm light. The 594-nm light for imaging was illuminating the sample the entire time, except for the brief periods of 407-nm activation. Height of the image is 80 μm. (False color: red is the white-light transmission image and green are the fluorescence images, excited at 594 nm.)

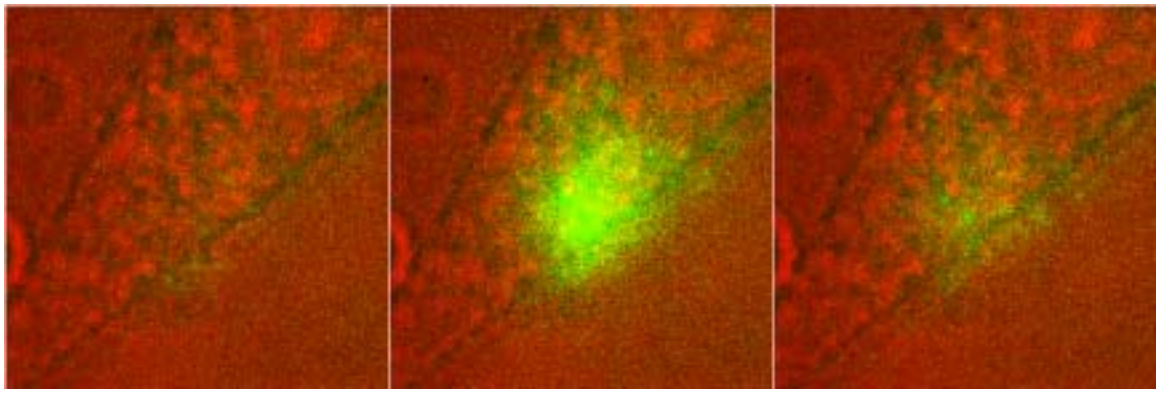

Figure S3. A CHO cell (500×) incubated with fluorogen **1** before (*left*), immediately after (*middle*), and 18.7 s after (*right*) a three-second activation with a tightly focused, moderate-irradiance (35 W/cm^2) 407-nm spot. The 594-nm light for imaging was illuminating the sample the entire time, except for the brief period of 407-nm activation. Only fluorophores in a small region of the cell are turned on, then they diffuse away and bleach. Height of the image is 16 μm. (False color: red is the white-light transmission image and green are the fluorescence images, excited at 594 nm.)

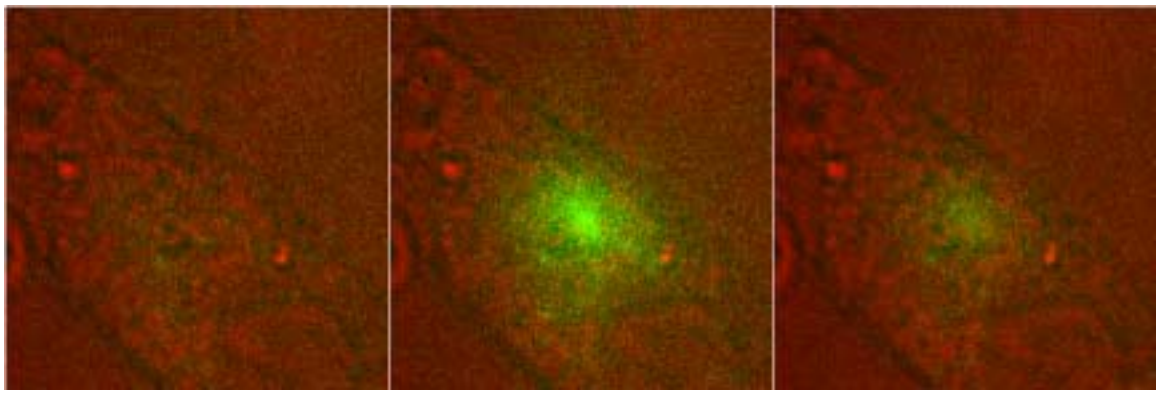

Figure S4. A CHO cell (500×) incubated with fluorogen **1** before (*left*), immediately after (*middle*), and 3.4 s after (*right*) a one-second activation with a tightly focused, moderate-irradiance (35 W/cm^2) 407-nm spot. The 594-nm light for imaging was illuminating the sample the entire time, except for the brief period of 407-nm activation. Only fluorophores in a small region of the cell are turned on, then they diffuse away and bleach. Height of the image is 16 μm. (False color: red is the white-light transmission image and green are the fluorescence images, excited at 594 nm.)

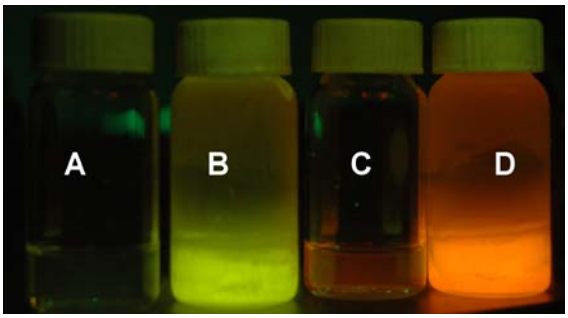

Figure S5. Equimolar samples of the fluorogen **1** kept in the dark (A–B) and after photoactivation (C–D) in liquid and frozen ethanol, illuminated at 365 nm (a 500-nm long-pass filter was placed before the lens of a digital camera in order to remove scattered excitation light and record only the fluorescence). The bright vials (B and D) are frozen. The red-shift is evident in the photoconverted samples. (For more information, see reference 3.)

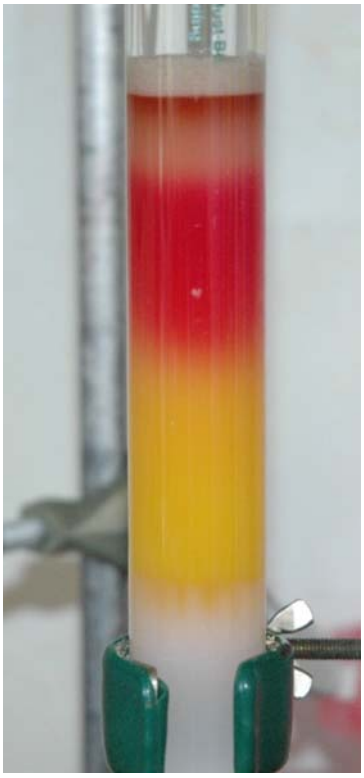

Figure S6. A photo of the silica-gel column separating photoproducts of irradiation of the azido-DCDHF **1**. The nitro species **3** (yellow band) eluted before the amine **2** (red band). See discussion below for details of separation and chemical analysis.

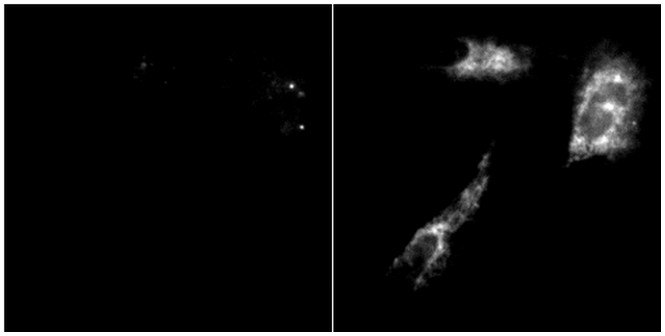

Figure S7. Fluorescence images only of cells in Figure 2. Transmission images not included.

Movie S1. Two confocal activations of fluorogen **1** in CHO. Imaging with 594 nm and activating with a one-second flash of tightly focused, moderate-irradiance (35 W/cm^2) 407-nm laser light; the activating frames are not included. One small area of the cell is activated, the focus is adjusted, the stage is moved laterally to a different area in the cell, and then another nearby spot is turned on. Single fluorophores can be seen diffusing in the cell; the ones already present at the beginning of the movie are from previous activations. Bright areas that do not diffuse may be covalently linked to relatively fixed biomolecules after activation, as in structure **4**. (In real time: 50 frames/s.) Height of the movie is 16 μm.

Movie S2. Movie of the molecule in Figure S1, running in real time: 50 frames/s. Height of the movie is 6 μm.

Movie S3. Wide-field activation of fluorogen **1** in a CHO. Imaging with 594 nm and activating with diffuse, low-irradiance (700 mW/cm^2) 407-nm laser light (colored circles indicate when each laser is on). Fluorescence from **2** grows in as the activating laser illuminates the cell. (In real time: 50 frames/s.) Height of the movie is 16 μm.

Materials and Methods

Synthesis. Literature procedures were followed for the synthesis of the precursors 4-azidobenzaldehyde[14] and 3-cyano-2-dicyanomethylene-4,5,5-trimethyl-2,5-dihydrofuran.[15] The 4-azidobenzaldehyde was isolated in 78% yield. Other reagents were commercially available and were used as received.

2-{4-(4'-Azidophenylethenyl)-3-cyano-5,5-dimethyl-5H-furan-2-ylidene}-malononitrile (**1**): The 4-azidobenzaldehyde (2.00 g, 13.6 mmol) and 3-cyano-2-dicyanomethylene-4,5,5-trimethyl-2,5-dihydrofuran (2.70 g, 13.6 mmol) were dissolved in 90 mL pyridine and a few drops of acetic acid were added. The mixture was stirred at room temperature for 24 h, poured into water, stirred for 30 min, kept in the refrigerator overnight, and then the precipitate was filtered off and air dried. The material was further purified by silica-gel column chromatography using hexane/EAC (7:3) as eluent and then finally recrystallized from dichloromethane/1-propanol to give the product as a solid (2.00 g, 44% yield). Mp 177–178 ºC; IR (neat, cm^{-1}) 3060, 2992, 2227, 2118, 1575, 1526, 1380; ^1H NMR (400 MHz, $CDCl_3$, δ): 7.61 (d, 2H, 8.4 Hz), 7.56 (d, 2H, J = 16.4 Hz), 7.09 (d, 2H, J = 8.4 Hz), 6.92 (d, J = 16.4 Hz, 2H), 1.77 (s, 6H); ^{13}C NMR (100 MHz, $CDCl_3$, δ) 174.5, 173.19, 145.65, 144.52, 130.48, 130.18, 119.84, 114.00, 111.27, 110.52, 109.94, 97.30, 26.23; UV–vis (CH_2Cl_2): λ_{max} = 433 nm; Anal. Calcd for $C_{18}H_{12}N_6O$: C, 65.85; H, 3.68; N, 25.60; Found: C, 65.58; H, 3.74; N, 25.94.

(*E*)-2-(4-(4-Aminostyryl)-3-cyano-5,5-dimethylfuran-2(5*H*)-ylidene)malononitrile (**2**):

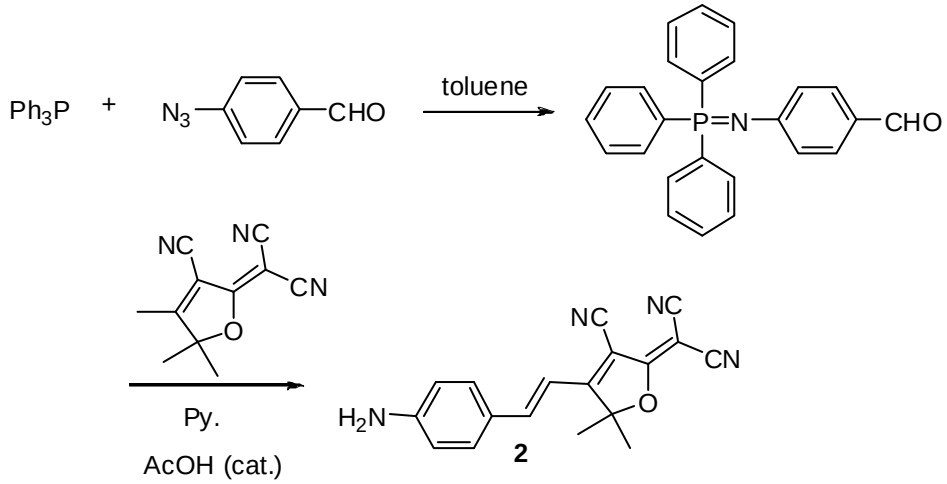

Triphenylphosphine (0.43 g, 1.6 mmol) and anhydrous toluene (12 mL) were added to a 100-mL two-neck round-bottom flask equipped with an additional funnel. The mixture was cooled in an ice-water bath. Next, 4-azidobenzaldehyde (0.30 g, 2.0 mmol) was dissolved in toluene (3 mL) in the additional funnel and added to the reaction mixture dropwise over 10 min. The reaction was continued at 0 ºC for 1 h. TLC showed complete conversion of 4-azido-benzaldehyde to one main product. The reaction was stopped and the solvent was removed by rotary evaporation. The remaining solid was recrystallized from 1-propanol and hexane to give the desired azaphosphane benzaldehyde as light yellow solid (0.54 g, 89% yield). IR (neat, cm^{-1}): 2965, 1660, 1586, 1504, 1463, 1338, 1156, 1105, 1010, 743, 719; ^1H NMR (400 MHz, $CDCl_3$, δ): 9.71 (s, 1H), 7.81–7.72 (m, 6H), 7.63–7.47 (m, 11H), 6.82 (d, J = 8.8 Hz, 2H); ^{13}C NMR (100 MHz, $CDCl_3$, δ): 190.5, 132.6, 132.5, 132.3, 131.5, 129.0, 128.9, 123.2, 123.0. This material was of sufficient purity for conversion the amine.

The azaphosphane benzaldehyde (0.38 g, 0.001 mol), 2-(3-cyano-4,5,5-trimethyl-5*H*-furan-2-ylidene)-malononitrile (0.199 g, 0.001 mol), pyridine (8 mL), and acetic acid (0.2 mL) were added to a 100-mL round-bottom flask with stirbar. The mixture was warmed to 40 ºC and kept at this temperature for 3 days and the reaction was monitored several times by TLC, which showed one purple product with high polarity was formed as the main product. The reaction was stopped and solvent was removed by rotary evaporation. The remaining solid was poured into ice water (200 mL) and stirred for 3 h. The precipitate was filtered off by suction filtration and recrystallized from a mixture of 1-propanol and dichloromethane to give the desired title compound as purple solid (0.23 g, 77% yield). Mp 360 ºC; IR (neat, cm^{-1}): 3487, 3366, 2229, 1643, 1519, 1496, 1265, 1169, 1111, 836; ^{1}H NMR (400 MHz, DMSO, δ): 7.88 (d, J = 16.0 Hz, 1H), 7.68 (d, J = 8.8 Hz, 2H), 6.86 (broad s, 2H), 6.82 (d, J = 16.0 Hz, 1H), 6.66 (d, J = 8.8 Hz, 2H), 1.74(s, 6H); ^{13}C NMR (100 MHz, $CDCl_3$, δ): 177.9, 176.1, 155.8, 150.4, 134.1, 122.5, 114.7, 114.0, 113.2, 112.6, 108.2, 98.6, 92.0, 51.1, 26.1; UV–vis (CH_2Cl_2): λ_{max} = 500 nm, ε = 3.1×10^4 M^{-1} cm^{-1}.

(*E*)-2-(3-Cyano-5,5-dimethyl-4-(4-nitrostyryl)furan-2(5*H*)-ylidene)malononitrile (**3**):

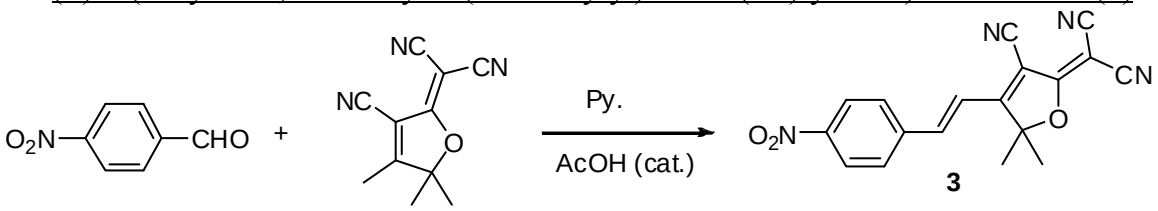

3

To a 100-mL round-bottom flask with stirbar was added 4-nitrobenzaldehyde (0.30 g, 0.002 mol), 2-(3-cyano-4,5,5-trimethyl-5*H*-furan-2-ylidene)-malononitrile (0.44 g, 0.0022 mol), pyridine (5 mL), and acetic acid (several drops). The reaction mixture was reacted at room temperature for 24 h. TLC showed that an orange product had been formed as the main product, but a small amount of 4-nitrobenzaldehyde still remained. The reaction was warmed to 40 ºC and continued for another 24 h. The reaction was stopped and cooled to room temperature. The reaction mixture was poured into ice water (500 mL) and stirred for 4 h. The brown precipitate was isolated by suction filtration and recrystallized from 1-propanol to give the desired product as a light brown powder (0.40 g, 67% yield). Mp 281 ºC; IR (neat, cm^{-1}): 3084, 2220, 1581, 1521, 1345, 1105; ^{1}H NMR (400 MHz, $CDCl_3$, δ): 8.34 (d, J = 8.8 Hz, 2H), 7.80 (d, J = 8.8 Hz, 2H), 7.68 (d, J = 16.8 Hz, 1H), 7.12 (d, J = 16.4 Hz, 1H), 1.83 (s, CH_3, 6H); ^{13}C NMR (100 MHz, $CDCl_3$, δ): 171.9, 149.6, 143.2, 139.4, 129.3, 124.6, 118.5, 110.9, 110.1, 109.6, 97.7, 26.2.

Chemical analysis of photoproducts. Samples for bulk chemical studies were photoconverted, both with and without removing dissolved oxygen by bubbling N_2, and analyzed using NMR and HPLC–MS. Samples of the azido-DCDHF **1** that were left in the dark were stable for months.

Column chromatography and NMR: A solution of photoconverted azido-DCDHF **1** in ethanol was separated on a TLC plate (1:3 acetone:dichloromethane) into two bands: a red band with lower R_f that was fluorescent under UV light (365 nm) and a yellow band with higher R_f that was nonemissive; the yellow band was not present when the solution of **1** was deoxygenated by bubbling N_2 before and during photoconversion. (Adequate separation was not achievable using dichloromethane and hexanes or dichloromethane alone; therefore, we resorted to acetone in the mobile-phase solvent mixture.)

For column chromatography, the photoproducts were separated on a column using silica gel as the stationary phase and 2:1 hexanes:acetone as the mobile-phase solvent. Two bands were well separated (see Figure S6): a yellow band of nitro **3** eluted first, then a red band of amine **2**

eluted later. NMR spectra of column-separated photoproducts confirm these identifications, as compared to pure, synthesized samples (although the yellow band was contaminated with some other minor photoproducts):[16, 17]

Compound **1**: ^{1}H NMR (400 MHz, $CDCl_3$, δ): 7.65 (d, J = 8.4 Hz, Ar, 2H), 7.61 (d, J = 16 Hz, vinyl, 1H), 7.13 (d, J = 8.4 Hz, Ar, 2H), 6.97 (d, J = 16 Hz, vinyl, 1H), 1.80 (s, CH_3, 6H).

Compound **2** (photoconverted from **1**, column separated): ^{1}H NMR (400 MHz, $CDCl_3$, δ): 7.58 (d, J = 16 Hz, vinyl, 1H), 7.50 (d, J = 8.4 Hz, Ar, 2H), 6.80 (d, J = 16 Hz, vinyl, 1H), 6.70 (d, J = 8.8 Hz, Ar, 2H), 4.39 (s, NH_2, 2H), 1.76 (s, CH_3, 6H).

Compound **2** (pure synthesized independently): ^{1}H NMR (500 MHz, $CDCl_3$, δ): 7.58 (d, J = 16 Hz, vinyl, 1H), 7.50 (d, J = 8.5 Hz, Ar, 2H), 6.80 (d, J = 17 Hz, vinyl, 1H), 6.70 (d, J = 8.5 Hz, Ar, 2H), 4.39 (s, NH_2, 2H), 1.76 (s, CH_3, 6H).

Compound **3** (photoconverted from **1**, crude, column enriched): ^{1}H NMR (300 MHz, $CDCl_3$, δ): 8.34 (d, J = 8.7 Hz, Ar), 7.80 (d, J = 8.4 Hz, Ar), 7.69 (d, J = 11 Hz, vinyl), 7.12 (d, J = 14 Hz, vinyl), 1.83 (s, CH_3).

Compound **3** (pure synthesized independently): ^{1}H NMR (400 MHz, $CDCl_3$, δ): 8.34 (d, J = 8.8 Hz, Ar, 2H), 7.80 (d, J = 8.8 Hz, Ar, 2H), 7.68 (d, J = 16.8 Hz, vinyl, 1H), 7.12 (d, J = 16.4 Hz, vinyl, 1H), 1.83 (s, CH_3, 6H).

Purification of **2** and **3** by semi-prep HPLC: An ethanolic solution containing ~1 mg/mL fluorogenic azide **1** was photoconverted using a 150-W Xe lamp for 5 min under air. Photoproducts **2** and **3** were separated by HPLC on a Hypersil Hyper Prep 100 BDS–C18 column (10.0×250 mm) with linear gradient elution (5–100% acetonitrile over 25 min, 5 min hold at 100% acetonitrile; balance by volume, 0.1 M tetraethylammonium acetate buffer, pH 7.5; total flow rate, 4 mL/min). The UV–vis absorption spectrum of the column eluent was continuously monitored using a Shimadzu diode array detector (SPD-M10A). Under these conditions, compounds **2** and **3** exhibited retention times of 20.9 and 22.5 min, respectively. No azide **1** (RT = 23.6 min) remained after photoactivation.

HPLC–MS characterization of photoproducts: Ethanolic solutions of **1** were photoconverted using diffuse 407-nm laser light under nitrogen (dissolved oxygen removed by bubbling N_2) or air. The photoactivation products were analyzed by HPLC–MS (Waters 2795 Separations module with 2487 Dual λ Absorbance Detector; Waters Micromass ZQ mass spectrometer). Gradient elution (2–95% acetonitrile with 0.1% formic acid over 20 min, 10 min hold at 95% acetonitrile/formic acid; balance by volume, water with 0.1% formic acid) through a C18 column (2.1×40 mm) was employed for the separation. The column eluent was subjected to electrospray ionization, and positive and negative ions with m/z from 100–1000 amu were detected.

In the absence of oxygen, photoconversion of **1** produced amine **2** (RT = 11.36 min; ESI^-: m/z = 301.7, $[M–H]^-$; ESI^+: m/z = 303.5, $[M+H]^+$) as the only major photoproduct. A putative azo dimer (RT = 16.97 min; ESI^-: m/z = 599.7, $[M–H]^-$) was observed as a minor photoproduct.

In air, photoactivation of **1** produced a mixture of amine **2** (RT = 11.43 min; ESI^-: m/z = 301.5, $[M–H]^-$; ESI^+: m/z = 303.4, $[M+H]^+$) and nitro **3** (RT = 12.99 min; ESI^-: m/z = 331.5, $[M–H]^-$, 315.5 $[M–O–H]^-$, 301.5 $[M–2O–H]^-$) as major products. After several days in air and room lights, an unidentified species believed to be generated from **3** formed in the solution (RT = 19.15 min; ESI^-: m/z = 367.6).

Bulk spectroscopy. Bulk solution absorption and emission spectra were acquired on a Perkin-Elmer Lambda 19 UV–vis spectrometer and a SPEX Fluoromax-2 fluorimeter using standard 1-

cm path length, quartz cuvettes. Absorption curves in Figure 1 of main text were smoothed with a moving average. Fluorescence quantum yields were referenced against standards with known quantum yields, corrected for differences in optical density and solvent refractive index.[18] Fluorophore **2** in ethanol was measured against Texas Red in ethanol (Φ_F = 0.93).[13] All quantitative measurements were done at low concentrations (absorbance values less than 0.2) to avoid any complications with dimer or aggregate formation. Molar absorption coefficients were measured from dilutions of solutions with known concentrations.

Sample preparation. Samples for aqueous bulk photostability measurements and quantitative single-molecule measurements were prepared using 5% (by mass) gelatin (type A, Bloom ~200, MP Biomedicals) in purified water. The gelatin solution was liquefied at 37 °C. A small volume (<0.5 μL) of dye stock solution in dimethyl sulfoxide was mixed with 10 μL gelatin, sandwiched between two Ar-plasma-etched glass coverslips, and allowed to gel at room temperature.

Polymer samples were prepared in 1% (by mass) solutions of poly(methyl methacrylate) (PMMA, T_g = 105 °C, MW = 75,000 g/mol, atactic, polydispersity ~2.8, PolySciences Inc.) in distilled toluene doped with nanomolar fluorophore concentrations; these solutions were then spin-cast onto Ar-plasma-etched glass coverslips to produce films 30 nm thick as measured by ellipsometry. (Distillation and plasma-etching were performed to remove fluorescent impurities.)

Microscopy. Samples were studied using an Olympus IX71 inverted microscope in an epifluorescence configuration[19] using 594-nm illumination from a HeNe laser (Meredith Instruments, 5 μW output); the irradiance at the sample was approximately 0.5–1.0 kW/cm^2. The emission was collected through a 100×, 1.4 N.A. oil-immersion objective, filtered using a 594RDC dichroic and HQ615LP long-pass filter (Chroma Technology) to remove scattered excitation light, and imaged onto an electron-multiplication Si EMCCD camera (Andor iXon+) with integration times of 20–100 ms. Photoactivation was performed using a 150-W Xe lamp or the 407-nm line from a Kr-ion laser (Coherent Innova-301); irradiances at the sample were generally less than 50 W/cm^2. Singles of **2** blinked more often than most secondary- and tertiary-amine DCDHFs. However, no oxygen scavengers were used for any imaging; including oxygen scavengers, triplet quenchers, or blowing with N_2 may reduce blinking, increase photostability, and reduce nonemissive photoproducts.[20-22]

Single-molecule photon-count analysis. All image analysis was performed using the ImageJ program (NIH). Single-molecule movies were used to extract the total number of detected photons before photobleaching, where all the photons (minus background) contributing to a single-molecule spot were spatially and temporally integrated. Results were plotted using the probability distribution of photobleaching: $P = m_N/M$, the ratio of the number of bleached singles m surviving after a given number of photons emitted N to the total number of molecules M in the measurement set.[23] This curve was fit using one or two exponential decays, and the decay constant was extracted from the fit (Equation 2). The probability-distribution approach for determining average photons emitted avoids any artifact from choice of bin size, and gives comparable results to histogramming.

The EM gain and conversion gain (defined as the number of A-to-D converter counts per photoelectron) were used to convert counts to photoelectrons; the linear EM gain was measured at various software settings, and the conversion gain from the manufacturer is 26.12 e^-/count. It is also useful to calculate the number of emitted photons $N_{tot,e}$ by correcting the measured value

of detected photons using the collection efficiency of our setup ($D = \eta_Q F_{coll} F_{opt} F_{filter}$), which is the product of the camera quantum efficiency η_Q, the angular collection factor F_{coll} determined by the objective NA, the transmission factor through the objective and microscope optics F_{opt}, and the transmission factor through the various filters F_{filter}, respectively.[19] At the emission wavelengths, η_Q = 92% for our camera, the maximum possible F_{coll} for our setup is 38% in PMMA and 45% in gelatin for a single dipole emitter aligned horizontally,[24] we measured F_{opt} for our setup to be 50%, and we measured F_{filter} to be 50% for the filter set we used. This yields D_{PMMA} = 8.7% and $D_{gelatin}$ = 10.3%.

Photobleaching and photoconversion quantum yields. The photobleaching quantum yield is defined as the probability of photobleaching after absorbing a photon, or the ratio of the bleaching rate R_B to the rate of absorbing photons R_{abs}:

$$\Phi_{B(P)} = \frac{R_{B(P)}}{R_{abs}} = \frac{1}{\tau_{B(P)} R_{abs}} = \frac{1}{\tau_{B(P)} \sigma_\lambda I_\lambda \left(\frac{\lambda}{hc} \right)}, \quad (1)$$

where $\tau_{B(P)}$ is the decay constant in the exponential fit, the absorption cross-section is related to the molar absorption coefficient by the equation $\sigma_\lambda = (1000)2.303\varepsilon_\lambda / N_A = 9.37 \times 10^{-17}$ cm^2 for compound **1**, I_λ is the irradiance at the sample, λ is the excitation wavelength, h is Planck's constant, and c is the speed of light. The average decay constant for a two-exponential fit, $F = \sum_{i=1}^{n=2} \alpha_i e^{(-t/\tau_i)}$, is given by:

$$\bar{\tau} = f_1 \tau_1 + f_2 \tau_2 = \frac{\alpha_1 \tau_1^{\,2} + \alpha_2 \tau_2^{\,2}}{\alpha_1 \tau_1 + \alpha_2 \tau_2}, \quad (2)$$

where $f_i = \alpha_i \tau_i \Big/ \sum_j \alpha_j \tau_j$ is the fractional area under the multi-exponential curve (see pages 141–143 of reference 18). (Some other papers use $t_{90\%}$, the irradiation time in seconds for 90% conversion to product, as a more practical measure than the decay constant $\bar{\tau}$;[25] compare values carefully.) Photobleaching quantum yield scales with the inverse of total number of photons emitted, and a lower value for Φ_B indicates better photostability.

Photoconversion by diffuse 407-nm laser light (3.1 mW/cm^2) was monitored by measuring changes over time in absorbance values of the reactant and photoproduct of interest in ethanol bubbled with N_2 (see Figure 1). The quantum yield of photoconversion Φ_P is defined in Equation 1 above, with τ_P as the average decay constant from the exponential fit of the decaying absorption values for the starting material. The fits in Figure 1 are [**1**] = $1.16e^{-t/7.40} + 1.50e^{-t/291} + 0.545$ (R^2 = 0.998) and [**2**] = $-2.32e^{-t/353} + 2.32$ (R^2 = 0.996). Note that Φ_P is the probability that the starting material will photoconvert for each photon absorbed; only a fraction of those photoconverted molecules become fluorescent (69% in ethanol).

Estimating photoconversion values for other systems. For calculating photoconversion and photoactivation values for other systems in Table S2, we used any available data published about the photoswitches to best estimate the values for Φ_P.

For Dronpa, we used figure 1h of reference 5, which reports a τ_P of 104 s when irradiated with 1 mW/cm^2 of 405-nm light. Using Equation 1, this yields Φ_P = 0.013. Although the original paper of Dronpa reports a Φ_P of 0.37, that calculation used a slightly different equation, which might account for the discrepancy. Moreover, using the activation curve in figure 1E of reference

4, we calculate an even smaller value (with I = 140 mW/cm^2 and $\tau_p \cong$ 3 s, the Φ_P is down to ~0.007). Also, our experience is that Dronpa requires significant doses of irradiation for photoswitching. Therefore, the estimate of Φ_P = 0.013 reported in Table S2 we believe to be reasonably accurate and fair. Note also that we report a value for Φ_B for Dronpa in Table S2 that is an order of magnitude smaller (i.e. better) than that in reference 4, because it has been demonstrated that singles can be reactivated many times.[5]

For PA-GFP, the supplemental material of reference 6 states to have used ~1 mW of 413-nm light in confocal mode; assuming 50% loss through the microscope, this is ~2×10^6 W/cm^2 at the sample. Using the same assumptions, we estimate the authors imaged using ~2 kW/cm^2 of 488-nm light, which is standard for confocal. Photoactivation was performed at these levels for ~1 s; assuming they only need a tenth of this time to activate, and τ_P = 0.1s, Φ_P would be ~3.3×10^{-8}. It is possible that the laser power of ~1 mW was used only for a confocal scan (and actually lower intensities were used for the 1-s activation); assuming a 1-ms/pixel scan rate, this would make Φ_P approximately 10^{-6}.

For reactivating EYFP singles, Dickson *et al.*[10] report irradiation for 5 min with a lamp using 1 W/cm^2 at 405 nm. These high doses of violet light coincide with our experience.

For the Cy3/Cy5 system, we extracted the slope of the plot of photoactivation rate versus intensity in figure 2b of reference 11 to estimate a value of Φ_P = 0.04, which is consistent with the claim in the same paper that singles can be switched using 1 s of 100-mW/cm^2 532-nm light.

We were unable to find enough information about the photochromism of rhodamine derivatives to estimate a Φ_P value, but reference 12 states that the system has a "low quantum efficiency of the photoinduced reaction."

Live-cell Imaging. For details of cell culture, see reference 26. CHO cells were plated on fibronectin-coated borosilicate chambered coverslips overnight prior to imaging. CHO cells were treated with 1-μM dye solution (1-mM dye stock in ethanol into growth medium) at 37 ºC for 1 hr, followed by extensive PBS buffer rinses to remove excess dye. Briefly, cells were imaged at 22 ºC in supplemented PBS buffer.[26] That is, imaging was performed within 45 min after removing the cell tray from the 37 ºC incubator to ensure cell viability.

For imaging, the irradiance of the 594-nm laser was 500 W/cm^2 for high-magnification cell images, and 20 W/cm^2 for low-magnification images; the 407-nm laser irradiance for photoactivation ranged from <1 to 35 W/cm^2.

Single-particle tracking in Figure S1 was performed using ImageJ and the "SpotTracker" plugin,[27] with the following parameters: maximum displacement of 5 pixels, intensity factor of 80%, intensity variation of 0%, movement constraint of 20%, and center constraint of 0%.

No changes in cell morphology were observed after photoactivation. Moreover, previous studies using DCDHFs in living cells did not encounter complications with toxicity.

References

(1) Anslyn, E. V.; Dougherty, D. A. In *Modern Physical Organic Chemistry;* University Science Books: Sausalito, CA, 2006.
(2) Hansch, C.; Leo, A.; Taft, R. W. *Chem. Rev.* **1991**, *91*, 165–195.
(3) Willets, K. A.; Nishimura, S. Y.; Schuck, P. J.; Twieg, R. J.; Moerner, W. E. *Acc. Chem. Res.* **2005**, *38*, 549–556.
(4) Ando, R.; Mizuno, H.; Miyawaki, A. *Science* **2004**, *306*, 1370–1373.
(5) Habuchi, S.; Ando, R.; Dedecker, P.; Verheijen, W.; Mizuno, H.; Miyawaki, A.; Hofkens, J. *Proc. Natl. Acad. Sci.* **2005**, *102*, 9511–9516.
(6) Patterson, G. H.; Lippincott–Schwartz, J. *Science* **2002**, *297*, 1873–1877.
(7) Schmidt, T.; Kubitscheck, U.; Rohler, D.; Nienhaus, U. *Single Molecules* **2002**, *3*, 327.
(8) Harms, G. S.; Cognet, L.; Lommerse, P. H. M.; Blab, G. A.; Schmidt, T. *Biophys. J.* **2001**, *80*, 2396–2408.
(9) Patterson, G.; Day, R.; Piston, D. *J. Cell Sci.* **2001**, *114*, 837–838.
(10) Dickson, R. M.; Cubitt, A. B.; Tsien, R. Y.; Moerner, W. E. *Nature* **1997**, *388*, 355–358.
(11) Bates, M.; Blosser, T. R.; Zhuang, X. *Phys. Rev. Lett.* **2005**, *94*, 108101-1–108101-4.
(12) Fölling, J.; Belov, V.; Kunetsky, R.; Medda, R.; Schönle, A.; Egner, A.; Eggeling, C.; Bossi, M.; Hell, S. W. *Angew. Chem., Int. Ed.* **2007**, *46*, 6266–6270.
(13) Soper, S. A.; Nutter, H. L.; Keller, R. A.; Davis, L. M.; Shera, E. B. *Photochem. Photobiol.* **1993**, *57*, 972–977.
(14) Bartoszewska, B.; Szczerek, I. *Organika* **1979**, 31-5.
(15) Moerner, W. E.; Twieg, R. J.; Kline, D. W.; He, M. Fluorophore Compounds and Their Use in Biological Systems. U.S. Patent Appl. 10/604,282, July 8, 2003.
(16) Soundararajan, N.; Platz, M. S. *J. Org. Chem.* **1990**, *55*, 2034–2044.
(17) Cline, M. R.; Mandel, S. M.; Platz, M. S. *Biochemistry* **2007**, *46*, 1981–1987.
(18) Lakowicz, J. R. *Principles of Fluorescence Spectroscopy*; Springer: New York, 2006.
(19) Moerner, W. E.; Fromm, D. P. *Rev. Sci. Instrum.* **2003**, *74*, 3597–3619.
(20) Rasnik, I.; McKinney, S. A.; Ha, T. *Nat. Meth.* **2006**, *3*, 891–893.
(21) Widengren, J.; Chmyrov, A.; Eggeling, C.; Lofdahl, P.; Seidel, C. *J. Phys. Chem. A* **2007**, *111*, 429–440.
(22) Aitken, C. E.; Marshall, R. A.; Puglisi, J. D. *Biophys. J.* **2008**, *94*, 1826–1835.
(23) Molski, A. *J. Chem. Phys.* **2001**, *114*, 1142–1147.
(24) Zander, C.; Enderlein, J.; Keller, R. A., Eds.; *Single-Molecule Detection in Solution: Methods and Applications*; Wiley–VCH: Berlin, 2002.
(25) Adams, S. R.; Kao, J. P. Y.; Tsien, R. Y. *J. Am. Chem. Soc.* **1989**, *111*, 7957–7968.
(26) Vrljic, M.; Nishimura, S. Y.; Moerner, W. E.; McConnell, H. M. *Biophys. J.* **2005**, *88*, 334–347.
(27) Sage, D. *IEEE Trans. Image Processing* **2005**, *14*, 1372–1383.

compound **1**

(400 MHz, $CDCl_3$)

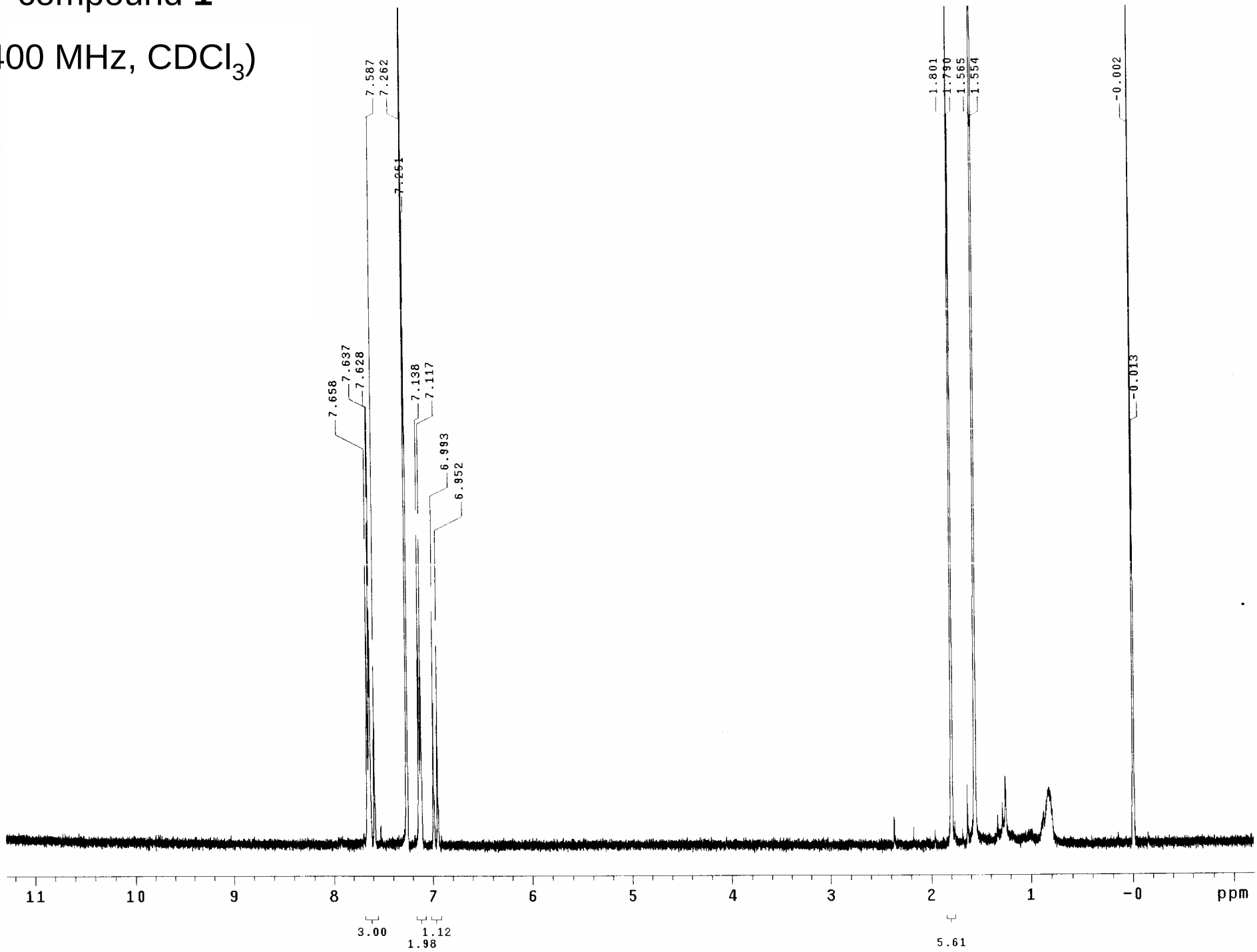

compound **1**

(400 MHz, $CDCl_3$)

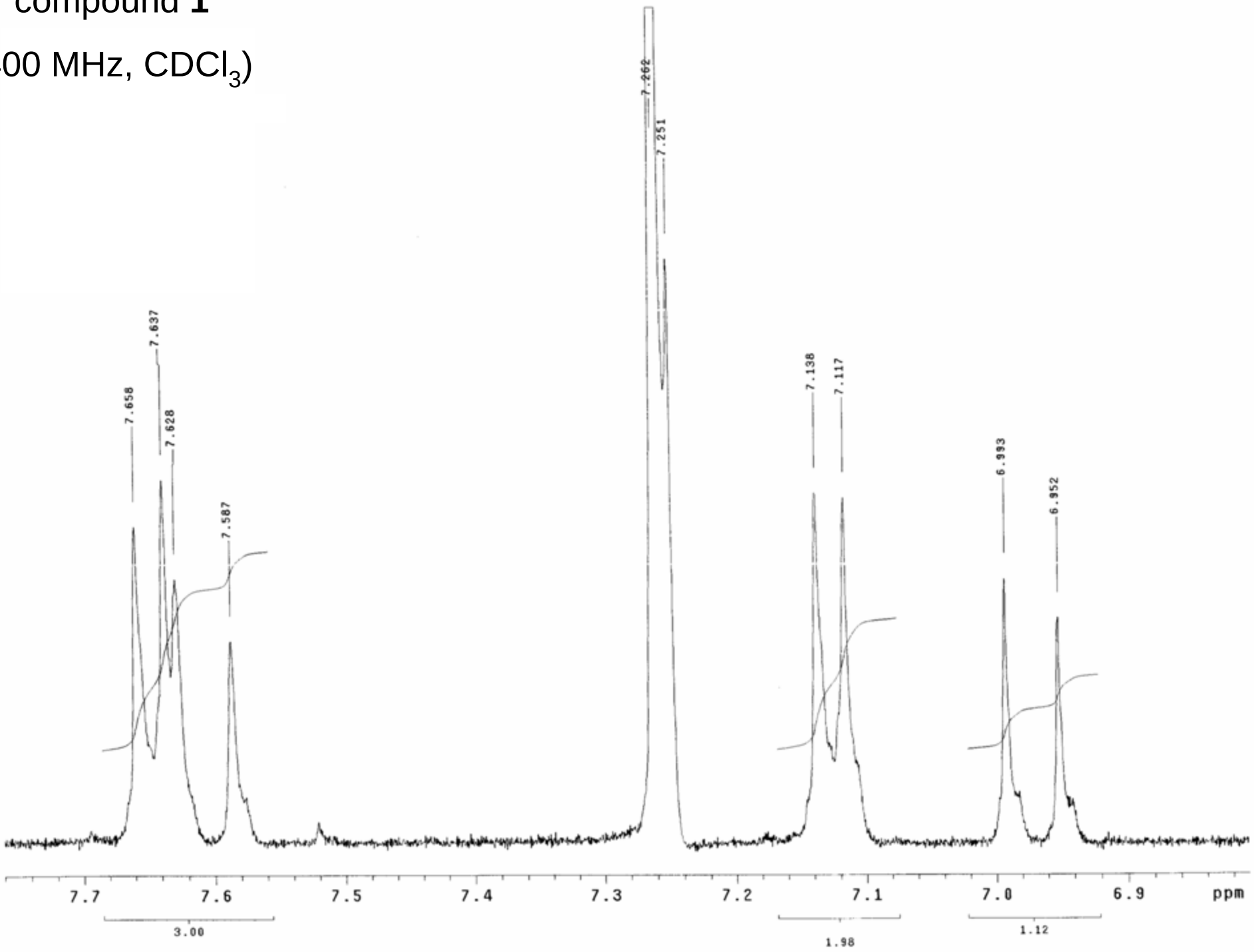

compound **1**

(400 MHz, $CDCl_3$)

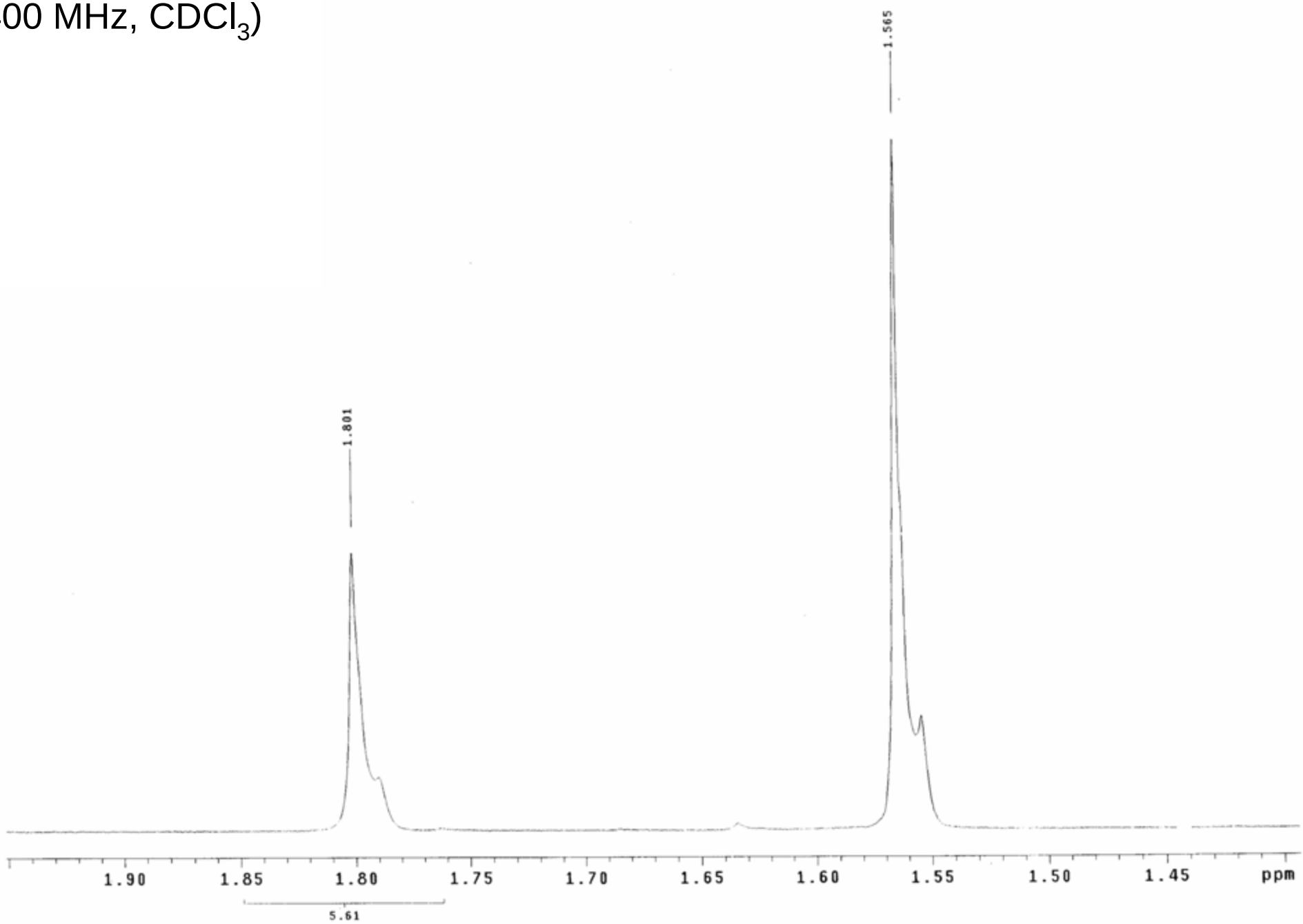

compound **2** (by photoconversion)

(400 MHz, $CDCl_3$)

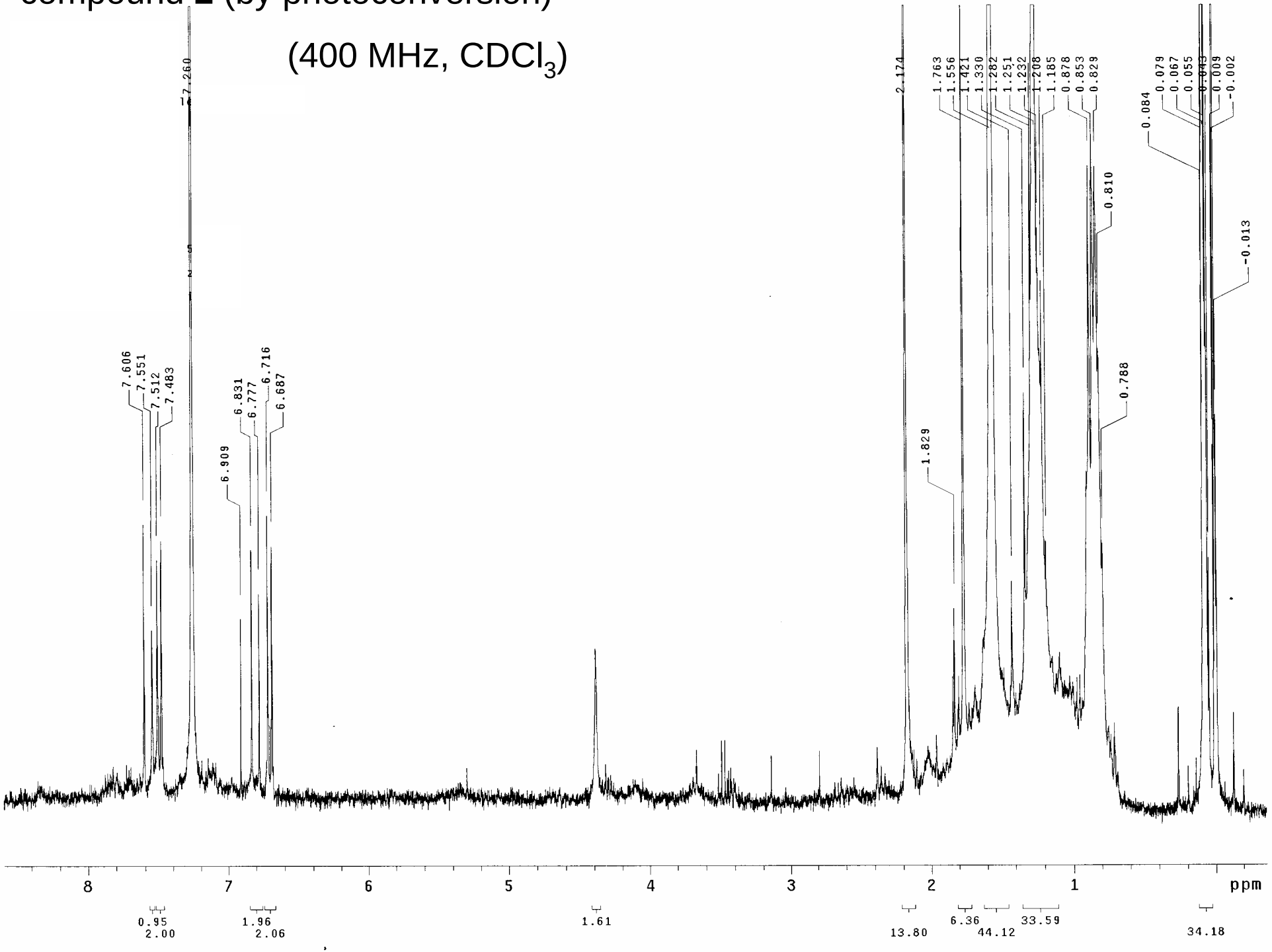

compound **2** (by photoconversion)

(400 MHz, $CDCl_3$)

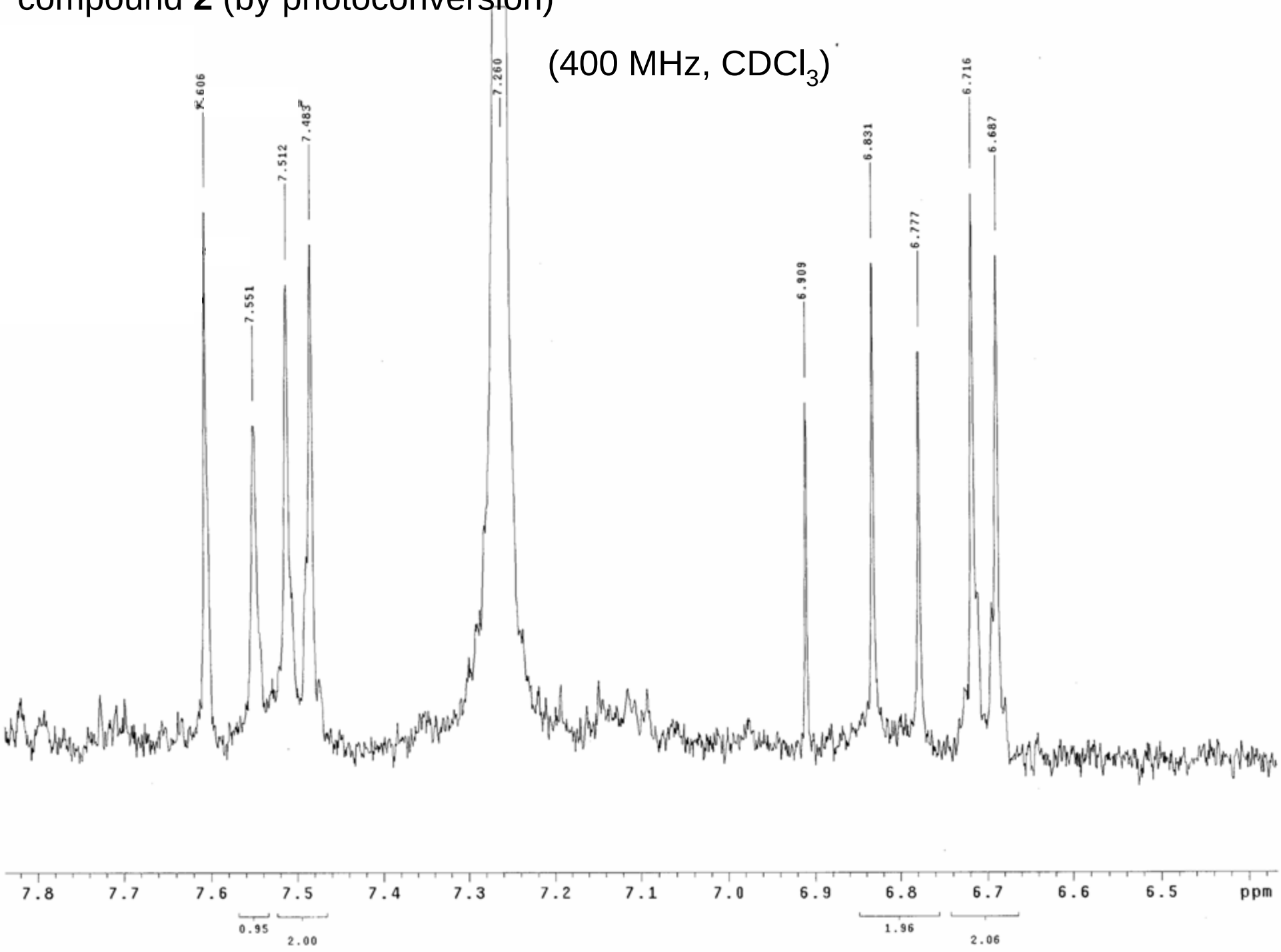

compound **2** (by photoconversion)

(400 MHz, $CDCl_3$)

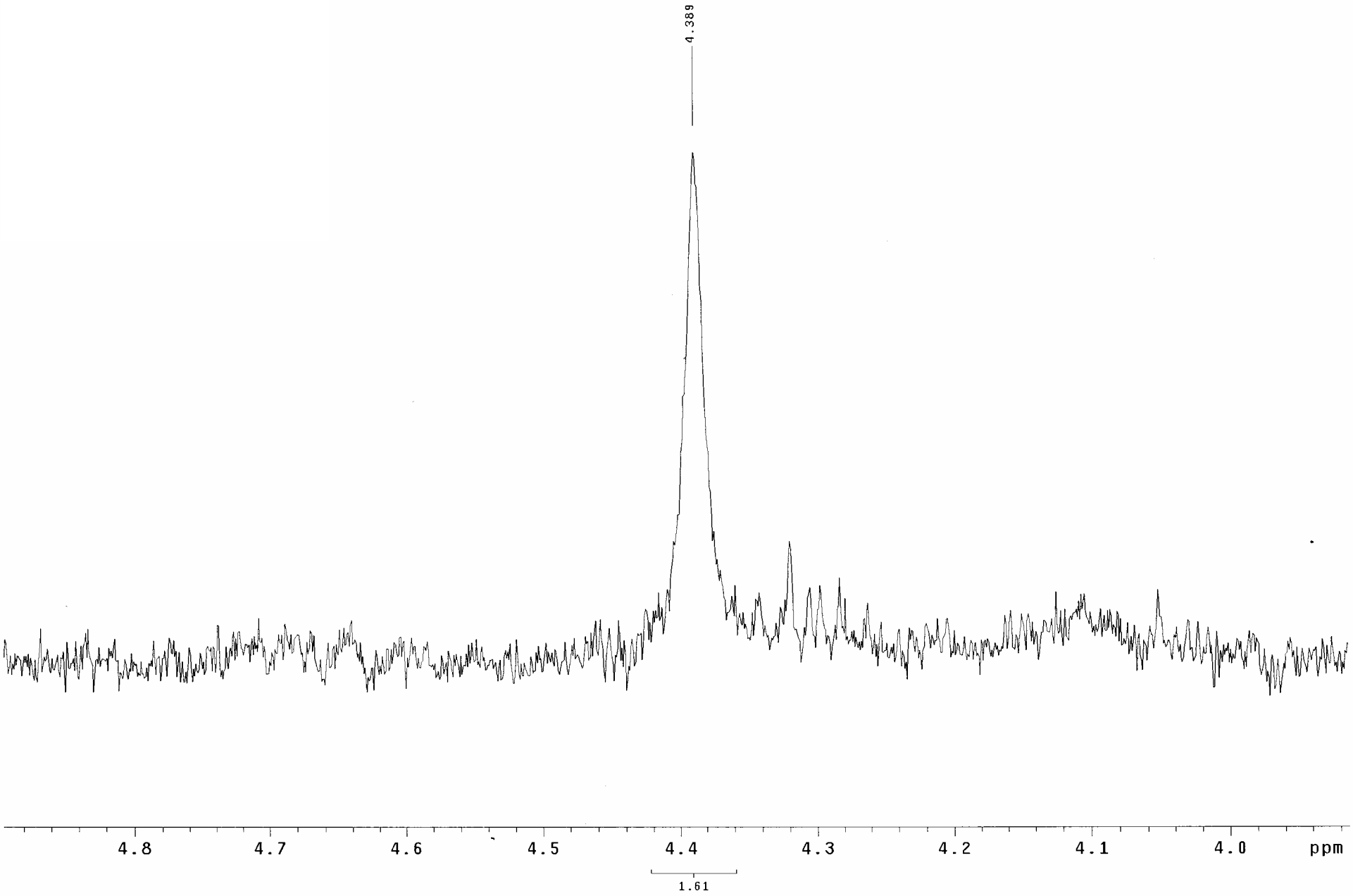

compound **2** (by photoconversion)

(400 MHz, $CDCl_3$)

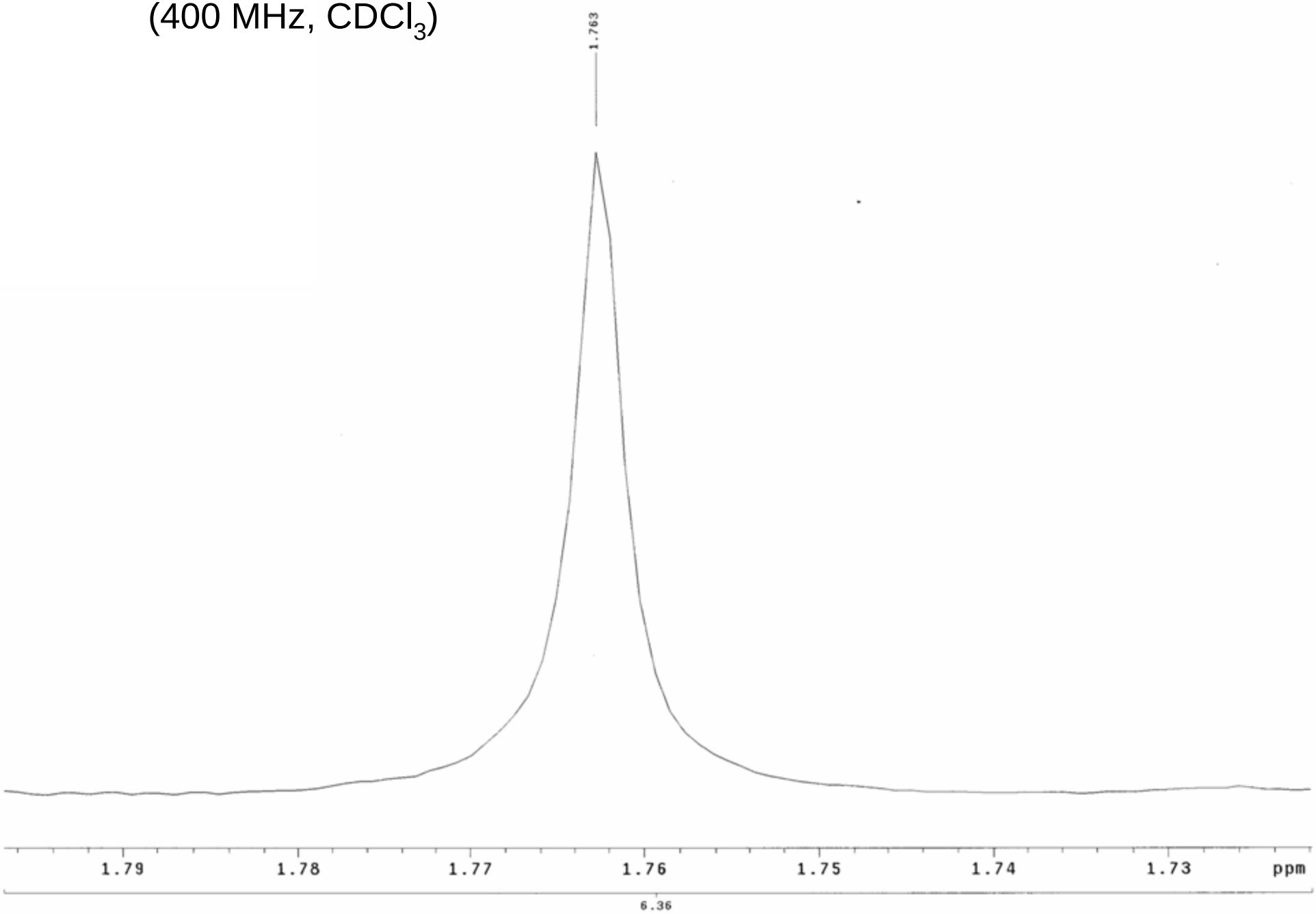

compound **2** (synthetic)

(500 MHz, $CDCl_3$)

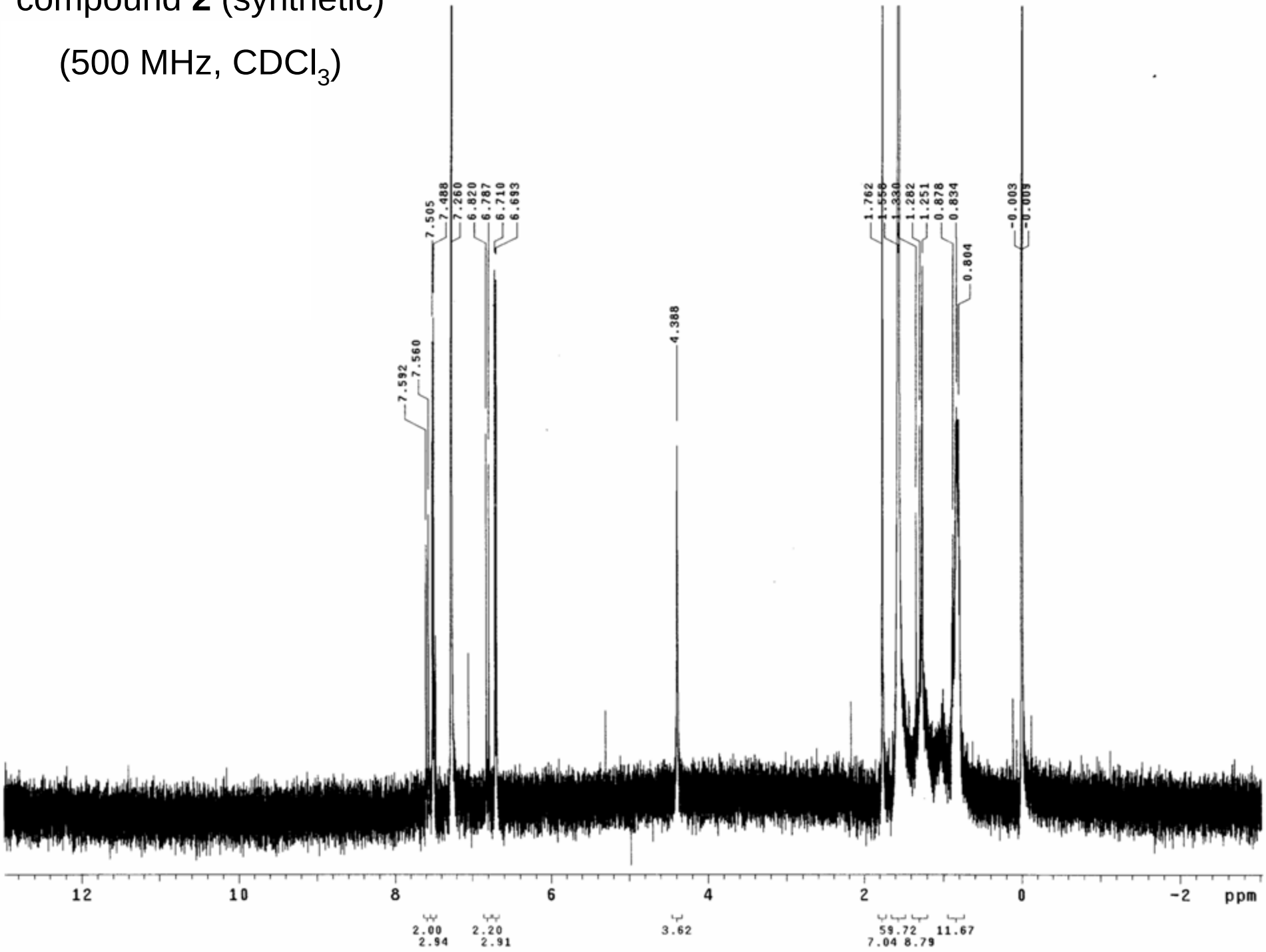

compound **2** (synthetic)

(500 MHz, $CDCl_3$)

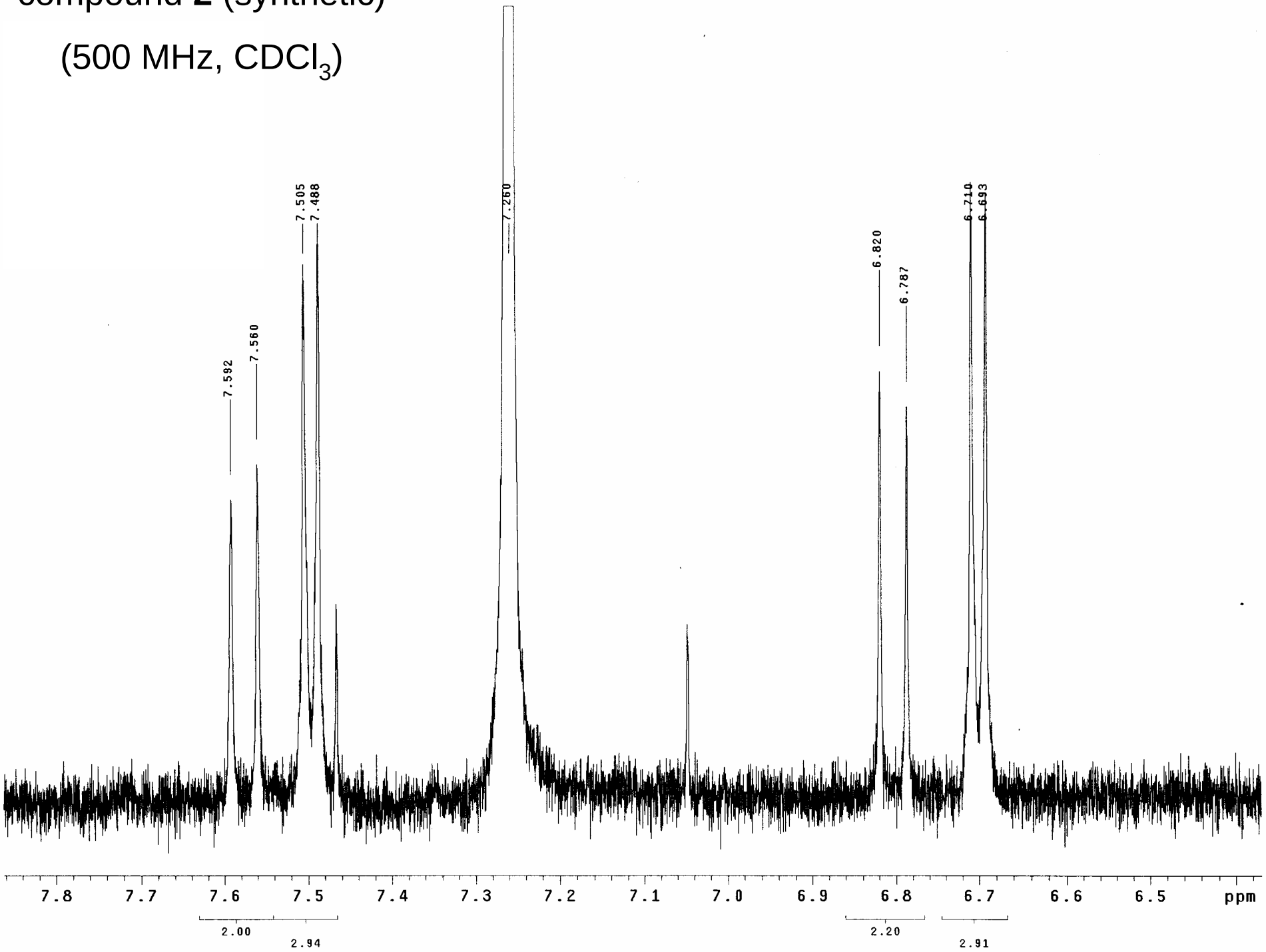

compound **2** (synthetic)

(500 MHz, $CDCl_3$)

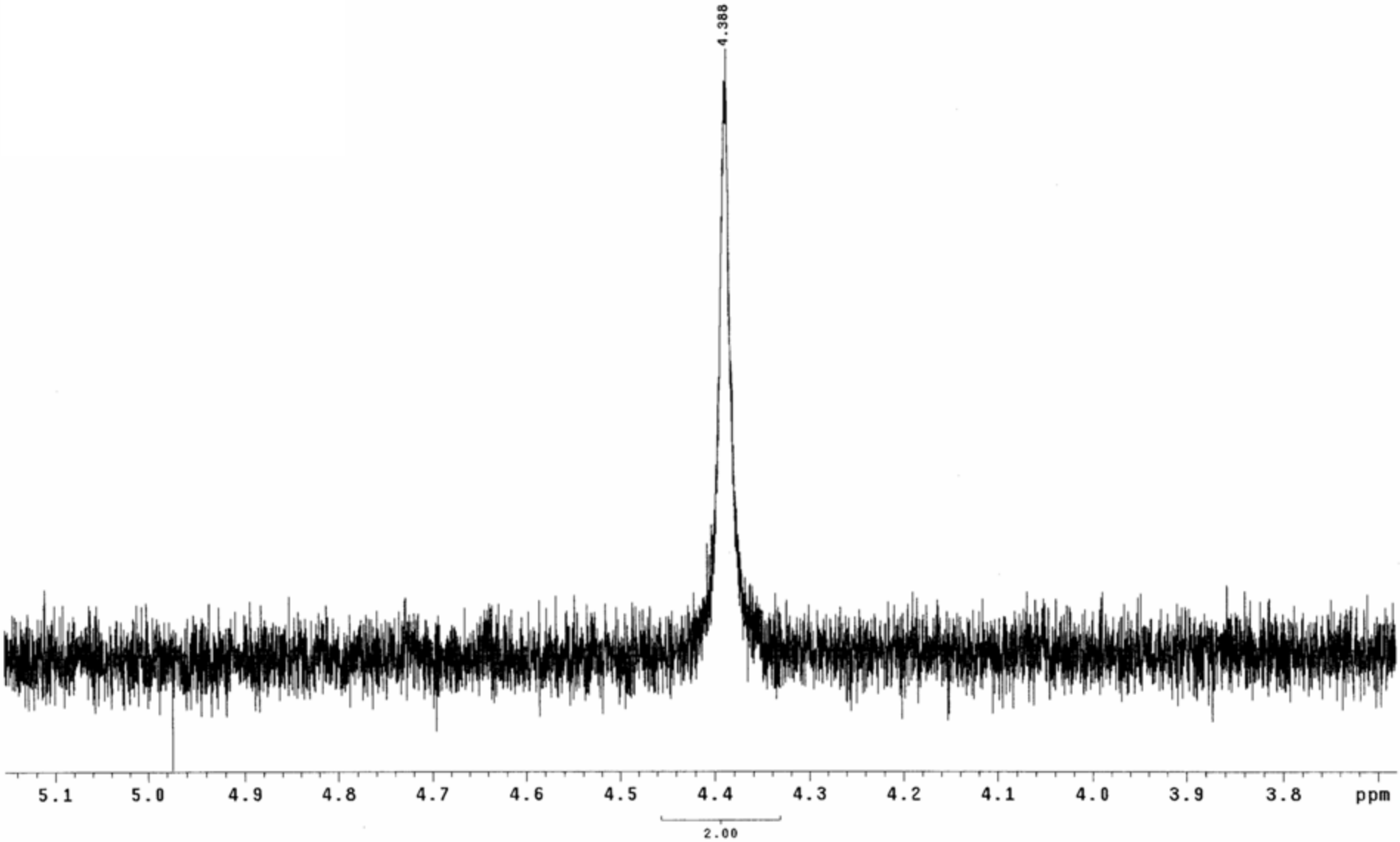

compound **2** (synthetic)

(500 MHz, $CDCl_3$)

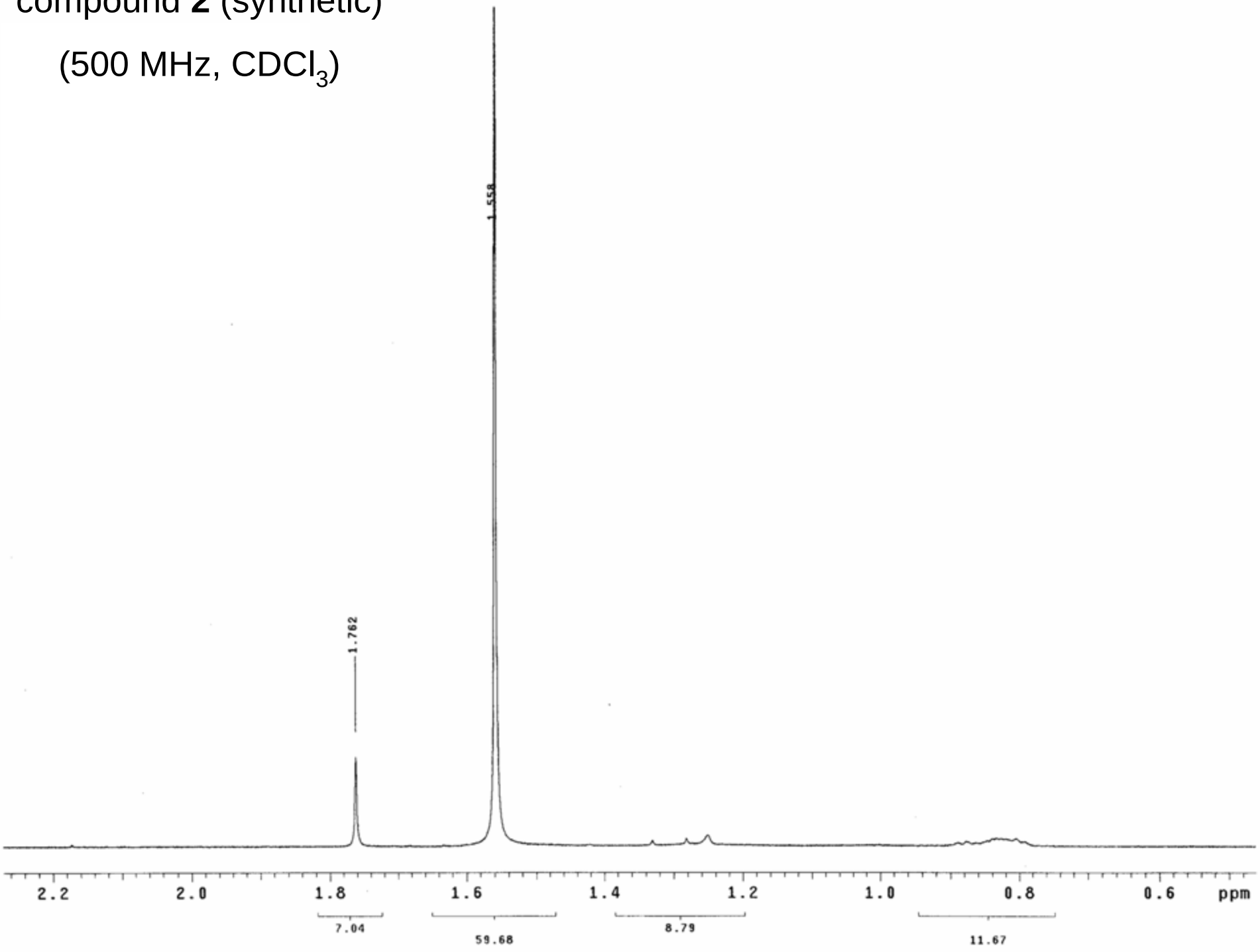

crude compound **3** (by photoconversion)

(300 MHz, $CDCl_3$)

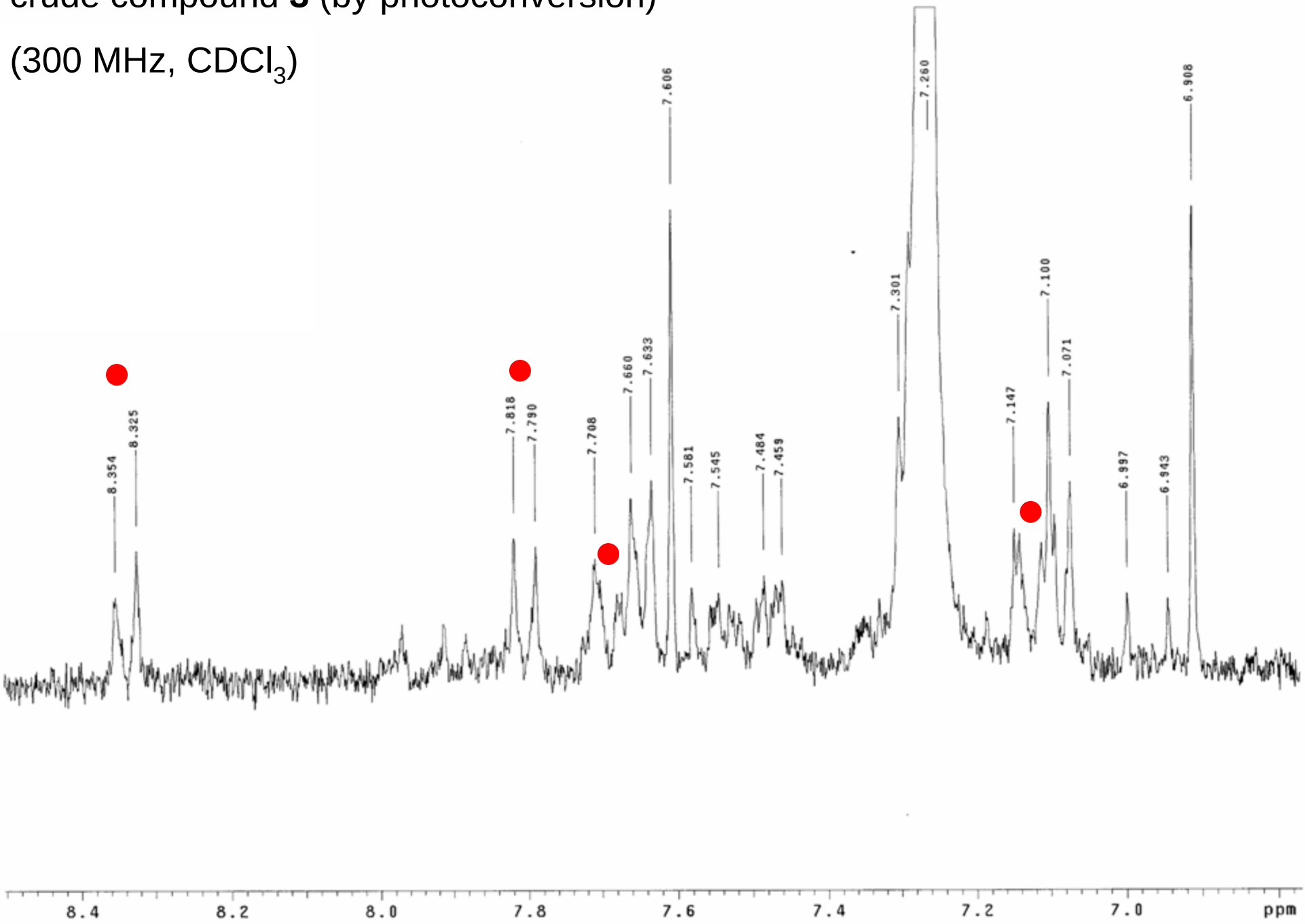

crude compound **3** (by photoconversion)

(300 MHz, $CDCl_3$)

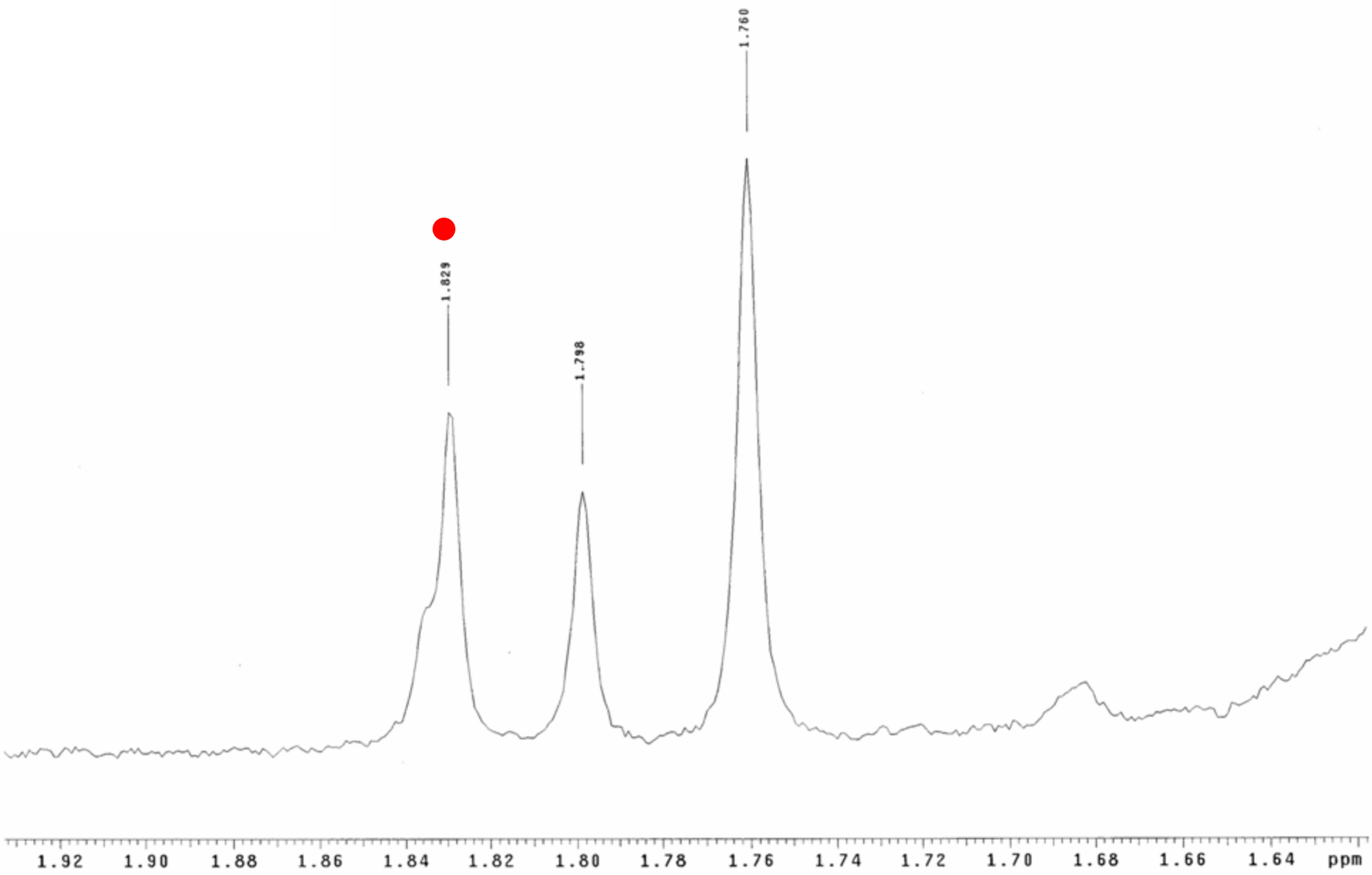

compound **3** (synthetic)

(400 MHz, $CDCl_3$)

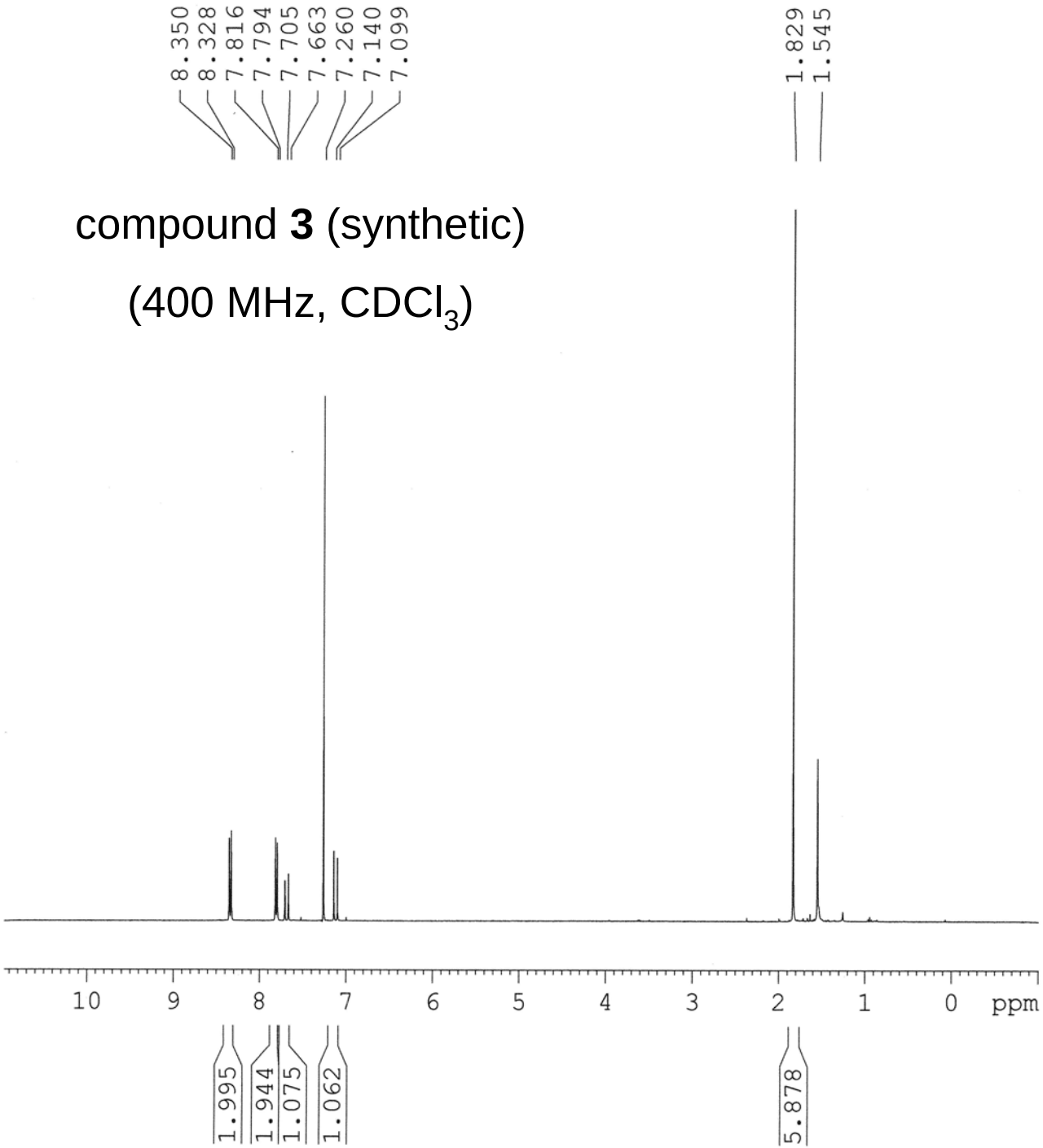


```
Current Data Parameters
NAME          Apr04-2008
EXPNO                 10
PROCNO                 1

F2 - Acquisition Parameters
Date_           20080404
Time               15.54
INSTRUM            spect
PROBHD   5 mm PABBO BB-
PULPROG               zg
TD                 16384
SOLVENT            CDCl3
NS                    16
DS                     0
SWH             4789.272 Hz
FIDRES          0.292314 Hz
AQ              1.7105396 sec
RG                 322.5
DW                104.400 usec
DE                  6.00 usec
TE                296.5 K
D1           10.00000000 sec
TD0                    1

======== CHANNEL f1 ========
NUC1                  1H
P1                  9.25 usec
PL1                -3.00 dB
SFO1        400.1320007 MHz

F2 - Processing parameters
SI                 16384
SF          400.1300104 MHz
WDW                   no
SSB                    0
LB                  0.00 Hz
GB                     0
PC                  1.00
```

compound **3** (synthetic)

(400 MHz, $CDCl_3$)

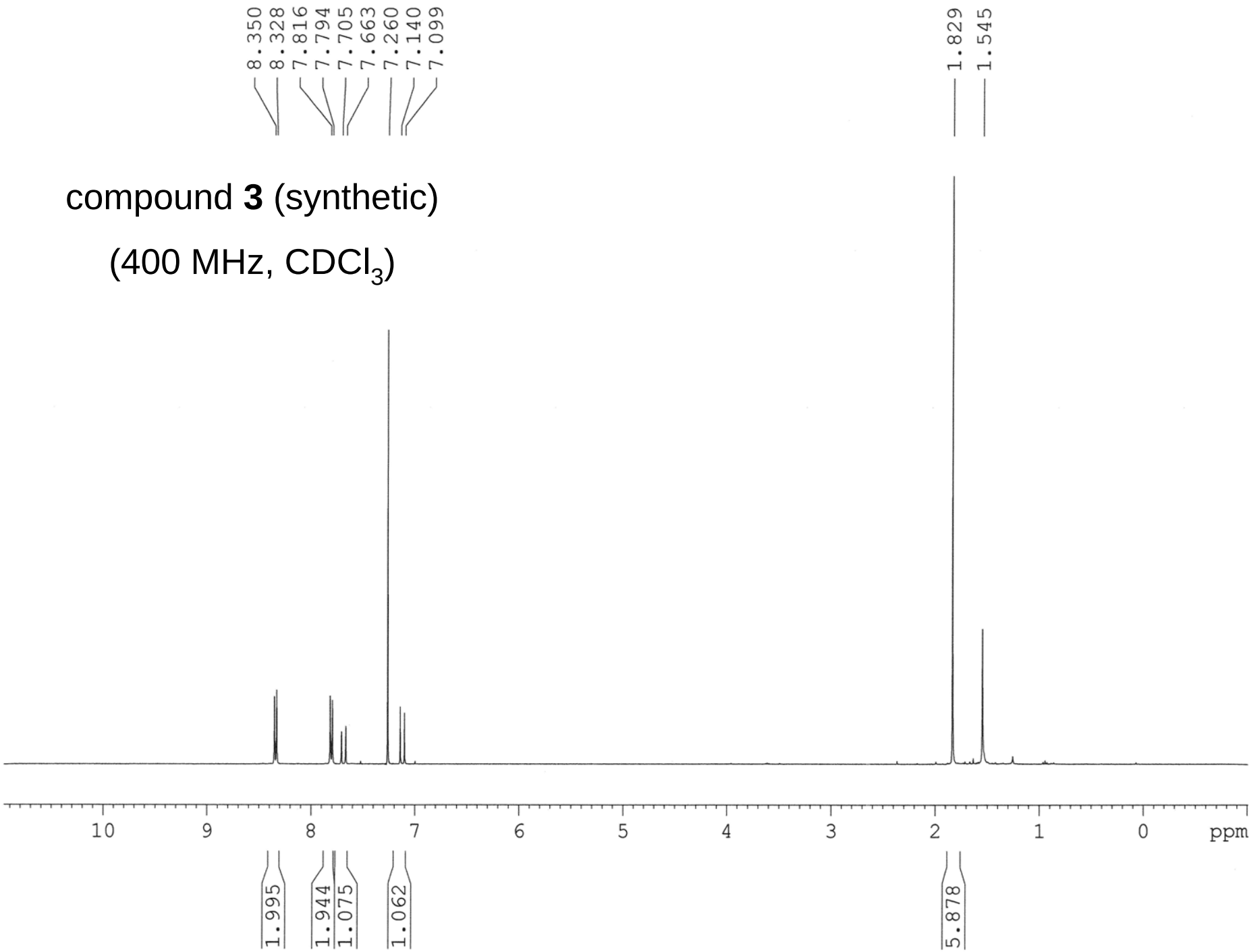

compound **3** (synthetic)

(400 MHz, $CDCl_3$)

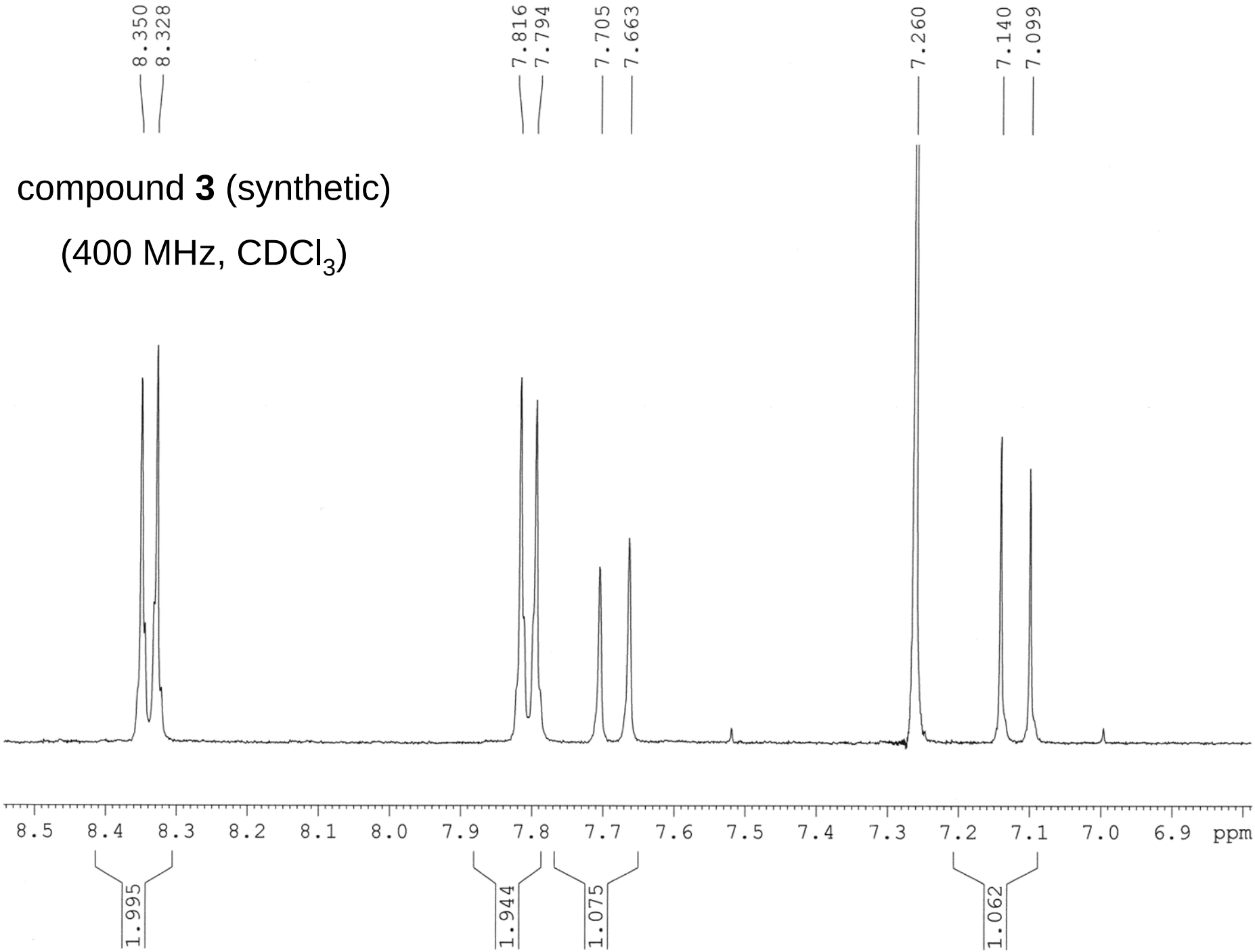

compound **3** (synthetic)

(400 MHz, $CDCl_3$)